

A Self Assembled Nanoelectronic Quantum Computer Based on the Rashba Effect in Quantum Dots

S. Bandyopadhyay*

Department of Electrical Engineering
University of Nebraska
Lincoln, Nebraska 68588-0511, USA

Abstract

Quantum computers promise vastly enhanced computational power and an uncanny ability to solve classically intractable problems. However, few proposals exist for robust, solid state implementation of such computers where the quantum gates are sufficiently miniaturized to have nanometer-scale dimensions. Here I present a new approach whereby a complete computer with nanoscale gates might be self-assembled using chemical synthesis. Specifically, I demonstrate how to self-assemble the fundamental unit of this quantum computer – a 2-qubit universal quantum gate – based on two exchange coupled multilayered quantum dots. Then I show how these gates can be wired using thiolated conjugated molecules as electrical connectors. Each quantum dot in this architecture consists of ferromagnet-semiconductor-ferromagnet layers. The ground state in the semiconductor layer is spin split because of the Rashba interaction and the spin splitting energy can be varied by an external electrostatic potential applied to the dot. A spin polarized electron is injected into each dot from one of the ferromagnetic layers and trapped by Coulomb blockade. Its spin orientation encodes a qubit. Arbitrary qubit rotations are effected by bringing the spin splitting energy in a target quantum dot in resonance with a global ac magnetic field by applying a potential pulse of appropriate amplitude and duration to the dot. The controlled dynamics of the universal 2-qubit rotation operation can be realized by exploiting the exchange coupling with the nearest neighboring dot. The qubit (spin orientation) is read via the current induced between the ferromagnetic layers under an applied potential. The ferromagnetic layers act as “polarizers” and “analyzers” for spin injection and detection. A complete prescription for initialization of the computer and data input/output operations is presented. This paradigm draws together two great recent scientific advances: one in materials science (nanoscale self assembly) and the other in information science (quantum computing).

*Corresponding author. E-mail: bandy@quantum1.unl.edu

1 Introduction

There is significant current interest in quantum computers because they possess vastly enhanced capabilities accruing from quantum parallelism [1, 2]. Some quantum computing algorithms [3, 4] have been shown to be able to solve classically intractable problems. i.e. perform tasks that no classical algorithm could perform efficiently or tractably. Thus, it would be highly desirable to build quantum computers.

Experimental effort in realizing quantum computers has been geared towards synthesizing universal quantum logic gates from which quantum computers can be built. A universal gate is a 2 qubit-gate [5, 6, 7] and has basically two attributes. First, it allows arbitrary unitary rotations on each qubit and second, it performs the quantum controlled rotation operation whereby one of the qubits (the target qubit) is rotated through an arbitrary angle, if, and only if, the other qubit (the control qubit) is oriented in a specified direction. The orientation of the control qubit is left unchanged. It is this conditional dynamics of the controlled rotation operation that is challenging to implement experimentally.

Recently, it has been shown [8, 9, 10] that there exist universal fault-tolerant computers that can operate in a non-ideal noisy environment. They are usually a circuit composed of one- or two-qubit gates performing various unitary rotations on a qubit (e.g Hadamard, Pauli rotations through rational or irrational angles, etc.). They too can, in principle, be realized from the basic gate that we discuss here.

The most vexing problem in experimentally realizing quantum computers is the issue of decoherence. Qubits are coherent superpositions of two-level states and, as such, are delicate entities. Any coupling to the environment will destroy the coherence of the superposition state and corrupt the qubit. Were it not for the recent discovery of quantum error correcting codes [11] that can correct errors due to decoherence through the use of appropriate *software*, quantum computing would have remained a theoretician's pipedream.

In the past, atomic systems were proposed as ideal testbeds for experimental quantum logic gates because of the relatively long coherence times associated with the quantum states of trapped atoms and ions [12]. Experimental demonstrations of quantum logic gates were carried out in atomic systems [13, 14]. Recently, nuclear magnetic resonance (NMR) spectroscopy has been shown to be an attractive alternative [15, 16] and there has been some reports of experimental demonstrations involving NMR [17]. However, there are also some doubts regarding the efficacy of NMR based approaches when dealing with many qubits [18].

The major drawback of both atomic and NMR systems is of course that they are unwieldy, expensive and inconvenient. Solid state (especially nanoelectronic) implementations would be much more desirable because, after all, miniaturization is as important as any other objective and has been fuelling the micro- or nano-electronics revolution for the past four decades. One would like a quantum gate that is one nanometer long and not one meter long. The technology base that exists in the solid-state area with regards to miniaturization is unparalleled.

While it is understood that solid state systems will be preferable vehicles for quantum computation, it is also well-known that the phase memory time of charge carriers in solids

saturate to only a few nanoseconds as the lattice or carrier temperature is lowered to a few millikelvins [19] (this is caused by coupling of carriers to the zero-point motion of phonons). Thus, solid state implementations of quantum gates where the qubits are coupled to charge degrees of freedom will be always dogged by serious decoherence problems. Even though such systems have been proposed in the past [20, 21, 22], they will require clock speeds in the far infra-red frequency range to meet Preskill's criterion for fault-tolerant computing [23].

A possible solution of this problem is to use the spin degrees of freedom in solid state systems to encode qubits since the spin is not coupled to electromagnetic noise and hence should have much longer coherence times than charge. It has been shown that electronic and nuclear spins of phosphorus dopant atoms ^{31}P in silicon have very long spin-flip times (or the co-called T_1 times in the language of spectroscopy) of about an hour [24]. Consequently, nuclear spins of ^{31}P dopant atoms in silicon have been advocated as preferable vehicles for qubits [26, 25, 27]. However, the actual coherence time (or T_2 time) of electron spin in P-doped silicon may be on the order of a millisecond. Compound semiconductors may exhibit somewhat shorter spin coherence times, but spin coherence times as long as 100 ns have been experimentally demonstrated in n-type GaAs at the relatively balmy temperature of 5 K [28]. Thus, it is practical to contemplate solid state quantum computers based on single electron spins.

Not all semiconductors however are suitable hosts for qubits. Pyroelectric materials (uniaxial crystals without inversion symmetry) usually exhibit electric dipole spin resonance which can increase the spin flip rate significantly [29] by strongly coupling the spin to phonons. An advantage of quantum dots is that the spin-phonon interaction may be reduced because of a constriction of the phase space for scattering. Moreover, the phonon-bottleneck effect [30] may block phonon-induced spin-flip transitions. Another obvious strategy to increase the coherence time is to decrease the phonon population by reducing the temperature. The temperature must be low in any case since the time to complete a quantum calculation should not significantly exceed the thermal time scale \hbar/kT [31] irrespective of any other consideration.

Quantum gates based on spin polarized single electrons housed in quantum dots have been proposed by us in the past [32] and more recently by Loss and DiVincenzo [33]. Here we adopt a different idea - which is still based on spin-polarized single electrons - to provide a realistic paradigm for the realization of a *self-assembled* solid-state, nanoelectronic universal quantum gate.

2 A Self Assembled Universal Quantum Gate

We will first self assemble a regimented array of *tri-layered* cylindrical quantum dots using an electrochemical technique to be described later. The two outer layers are ferromagnetic and the middle layer is a semiconductor (see Fig. 1).

A dc potential pulse is applied between the two outer (ferromagnetic) layers to inject a

single spin-polarized electron from one of the outer layers into the middle layer. Such spin polarized injection has been demonstrated in the CdMnTe-CdTe system which is shown in Fig. 1(b) [34]. In the middle layer, the electron's ground state is spin-split because of Rashba interaction [35, 36, 37]. The Rashba effect arises from spin-orbit coupling in the presence of a transverse electric field which is always present at the interface of two dissimilar materials owing to the conduction band discontinuity. It is possible to electrostatically *modulate* this spin splitting [39] by applying a potential between the two outer layers. The applied potential alters the interface field that causes the Rashba effect and hence changes the spin-splitting energy. As long as this potential is less than $e/2C$ (e is the electron charge and C is the dot's capacitance) we can change the spin splitting *without* inducing a current flow (causing the injected electron to escape), or causing another electron to be injected. In other words, the electron is trapped in the middle layer of the quantum dot by Coulomb blockade and the applied potential only varies the spin splitting energy.

The trapped electron can be injected into the semiconductor quantum dot with a spin polarization that is an exact eigenspinor state. This is achieved by magnetizing the ferromagnetic injecting contact in the appropriate direction. A globally applied ac magnetic field which resonates with the spin-splitting energy will then couple the electron to both spin states and the electron will exist in a coherent superposition of the two eigenspinors, thus forming a qubit. A target qubit is selected for rotation by bringing its spin-splitting energy in resonance with the external global ac magnetic field by applying a suitable potential pulse between that particular dot's ferromagnetic outer layers. This varies the spin-splitting energy via the Rashba effect. Arbitrary qubit (spin) rotation is achieved by varying the pulse duration, i.e. the duration of resonance with the ac magnetic field. Such a procedure realizes the first ingredient of a universal quantum gate, namely arbitrary single qubit rotations.

In order to achieve the second and last ingredient of a universal quantum gate - namely the conditional dynamics of a universal 2-qubit gate - we need to couple the rotation of one qubit (target qubit) with the orientation of another qubit (control qubit). This can be done by exploiting the exchange coupling between two single electrons in two neighboring dots. The spin-splitting energy in any dot depends, among other things, on the spin orientation in the neighboring dot if the two dots are exchange coupled. The exchange coupling can be varied by simultaneously applying two independent potentials to the target and control qubits. Thus, the conditional dynamics of the controlled rotation operation can be achieved.

Finally, we have to "read" a qubit for data output. The qubit (spin orientation in a dot) is read directly via the current induced between the dot's spin polarized outer layers (ferromagnetic contacts) when a sufficiently strong potential is applied to overcome the Coulomb blockade. The magnitude of the current tells us the electron's spin orientation because it depends on the angle between the electron's spin orientation and the direction of magnetization in the ferromagnetic contact (which is known *a priori*). This principle was prescribed for measuring spin precession in the so-called spin-transistor proposed more than ten years ago [37]. The single electron current is small, but can be measured using sensitive electrometers.

2.1 Rashba effect in a quantum dot

The Hamiltonian for the Rashba interaction is given by

$$H_R = -i \left[\vec{\sigma} \times \vec{\nabla} \right] \cdot (\alpha_\nu \hat{\nu}) = \left[\vec{\sigma} \times \frac{\vec{p}}{\hbar} \right] \cdot (\alpha_\nu \hat{\nu}) , \quad (1)$$

where $\vec{\sigma}$ is the Pauli spin matrix, \vec{p} is the momentum operator, $\hat{\nu}$ is the unit vector normal to the interface and α_ν is the coupling constant along the ν -axis which is proportional to the expected value of the interface electric field along the ν -axis [36].

We will use the coordinate system shown in Fig. 1. For mathematical convenience, the quantum dot will be assumed to have a rectangular shape with the dimension along the x-direction much larger than the dimensions along the y- and z-directions. Such a dot is appropriately referred to as a quantum “dash” and is a realistic representation for quantum dots synthesized by the type of self-assembly that we will propose.

The Rashba interaction will distort the wavefunction (particle-in-a-box state) of the lowest subband in each dot by causing mixing of the unperturbed subbands. If the dimensions of the quantum dash are small enough that the subbands are well separated in energy, then we can neglect most of the subband mixing and include only the perturbation of the second lowest (or nearest) subband on the lowest subband. This basically requires that the transverse widths of the quantum dash W_z and W_y be small enough that they are much smaller than the quantity $\hbar^2/\alpha m^*$ where m^* is the electron’s effective mass in the conduction band [37]. In compound semiconductors, the spin-orbit coupling coefficient α has been experimentally measured and found to be of the order of 10^{-12} eV-m [38]. Hence, we need W_z and W_y to be much smaller than about $0.5 \mu\text{m}$. In self-assembled structures, W_z and W_y are about 100 \AA so that we can easily neglect the mixing of transverse subbands (along the y- and z-directions) and include only the effect of the nearest longitudinal subband along the x-direction.

Based on the above consideration, the spatial part of ground state wavefunction of an isolated electron can be written as

$$\psi_{ground}(spatial) = \left(\frac{2\sqrt{2}}{W_x W_y W_z} \right) \left(\frac{1}{\sqrt{1 + |a|^2}} \right) \left[\sin\left(\frac{\pi x}{W_x}\right) + a \sin\left(\frac{2\pi x}{W_x}\right) \right] \sin\left(\frac{\pi y}{W_y}\right) \sin\left(\frac{\pi z}{W_z}\right) . \quad (2)$$

The above wavefunction is of course not exact since the electrons are not confined by hardwall boundaries. In fact, hardwall boundaries will not allow the wavefunctions of neighboring electrons to overlap and they need to do so in order to have any residual exchange interaction which is critical to the 2-qubit controlled rotation operation. However, Equation (2) serves as a good zeroth-order estimate for the wavefunction and allows us to evaluate spin eigenstates analytically.

We will assume that equal electric fields have been applied along the transverse (y- and z-directions) and also $\alpha_y = \alpha_z = \alpha$. The following analysis pertains to an isolated electron exchange decoupled from its neighbors.

The time-independent Schrödinger equation describing the ground state of the system is

$$H_0\psi_{ground} \begin{pmatrix} \mu \\ \nu \end{pmatrix} + H_R\psi_{ground} \begin{pmatrix} \mu \\ \nu \end{pmatrix} = E_{ground}\psi_{ground} \begin{pmatrix} \mu \\ \nu \end{pmatrix}, \quad (3)$$

where $(\mu \nu)$ is the spin eigenbra.

Multiplying Equation (3) by the eigenbra $\langle \psi_{ground}|$, we get

$$\begin{bmatrix} \langle H_0 \rangle + \langle H_R \rangle_{11} & \langle H_R \rangle_{12} \\ \langle H_R \rangle_{21} & \langle H_0 \rangle + \langle H_R \rangle_{22} \end{bmatrix} \begin{pmatrix} \mu \\ \nu \end{pmatrix} = E_{ground} \begin{pmatrix} \mu \\ \nu \end{pmatrix}, \quad (4)$$

where $\langle H_0 \rangle = (\hbar^2/2m^*)/[\eta(\pi/W_x)^2 + (\pi/W_y)^2 + (\pi/W_z)^2]$ $\eta = 1 + 4|a|^2/(1 + |a|^2)$.

The Rashba Hamiltonian is

$$H_R = \alpha \left[\sigma_z \frac{p_x}{\hbar} - \sigma_x \frac{p_z}{\hbar} + \sigma_x \frac{p_y}{\hbar} - \sigma_y \frac{p_x}{\hbar} \right] \quad (5)$$

so that

$$\langle H_R \rangle = \alpha \begin{bmatrix} \langle p_x \rangle / \hbar & i \langle p_x \rangle / \hbar \\ -i \langle p_x \rangle / \hbar & - \langle p_x \rangle / \hbar \end{bmatrix}, \quad (6)$$

where

$$\langle p_x \rangle = -i\hbar \left\langle \psi_{ground} \left| \frac{\partial}{\partial x} \right| \psi_{ground} \right\rangle = \frac{16\hbar}{3W_x} \frac{Im(a)}{1 + |a|^2}, \quad (7)$$

and $Im(a)$ is the imaginary part of a . Note that $\langle p_y \rangle = \langle p_z \rangle = 0$.

Substituting the result of Equation (6) into Equation (4), we get

$$\begin{bmatrix} \langle H_0 \rangle + \alpha \langle p_x \rangle / \hbar - E_{ground} & i\alpha \langle p_x \rangle / \hbar \\ -i\alpha \langle p_x \rangle / \hbar & \langle H_0 \rangle - \alpha \langle p_x \rangle / \hbar - E_{ground} \end{bmatrix} \begin{pmatrix} \mu \\ \nu \end{pmatrix} = 0. \quad (8)$$

Diagonalizing the above Hamiltonian yields the eigenenergies and eigenkets of the spin-split ground state:

$$\begin{aligned} E_{\uparrow} &= \langle H_0 \rangle + \frac{\sqrt{2}\alpha p_x}{\hbar} \\ E_{\downarrow} &= \langle H_0 \rangle - \frac{\sqrt{2}\alpha p_x}{\hbar}, \end{aligned} \quad (9)$$

The spin eigenstates associated with lowest spin-split levels (whose eigenenergies are given in Equation (8)) are (in spinor notation)

$$\begin{aligned} |\uparrow\rangle &= \begin{pmatrix} \sqrt{2} + 1 \\ -i \end{pmatrix} \\ |\downarrow\rangle &= \begin{pmatrix} \sqrt{2} - 1 \\ i \end{pmatrix} \end{aligned} \quad (10)$$

which are orthogonal to each other.

It is easy for the reader to verify that if we had applied the Rashba field in the y-direction, then the spin-split ground state would have been

$$\begin{aligned} E_{\uparrow} &= \langle H_0 \rangle + \frac{\alpha p_x}{\hbar} \\ E_{\downarrow} &= \langle H_0 \rangle - \frac{\alpha p_x}{\hbar}, \end{aligned} \quad (11)$$

and the eigenspinors would have been

$$\begin{aligned} |\uparrow\rangle &= \begin{pmatrix} 1 \\ 0 \end{pmatrix} \\ |\downarrow\rangle &= \begin{pmatrix} 0 \\ 1 \end{pmatrix} \end{aligned} \quad (12)$$

Thus, the y-directed Rashba field would have lifted the degeneracy between the +z-polarized and -z-polarized spins. Similary, if the Rashba field were applied along the z-direction, the spin-split eigenenergies would have been still given by Equation (11) and the eigenspinors would have been

$$\begin{aligned} |\uparrow\rangle &= \begin{pmatrix} 1 \\ -i \end{pmatrix} \\ |\downarrow\rangle &= \begin{pmatrix} 1 \\ i \end{pmatrix}. \end{aligned} \quad (13)$$

That is, the z-directed Rashba field would have lifted the degeneracy between the +y- and -y-polarized spins.

In all cases, since the Rashba splitting is proportional to α which depends on the applied electric field, it is possible to modulate the spin-splitting with a gate potential. This is critical to the operation of the quantum gate.

2.2 Coherent spin injection from spin polarized contacts

Assume that the ferromagnetic contacts to the quantum dots (the two outer layers) exhibit nearly 100% spin polarization and are permanently magnetized along one of the eigenspinor polarizations. It may be possible to obtain almost 100% spin polarization in half-metallic CrO₂ [40] and some other Heusler alloys such as half metallic (Co_{1-x}Mn_x)_{0.75}Ge_{0.25} which are ferromagnetic with a Curie temperature above room temperature. However, their interface with semiconductors (quantum dot material) may not be ideal. Recently, spin polarized hole injection was demonstrated from GaMnAs into GaAs [41] at around a temperature of 120 K. Prior to that, spin polarized injection from CdMnTe into CdTe was demonstrated [34], but the disadvantage in that case is that CdMnTe is not a permanent ferromagnet; the spin polarization needs to be maintained by a globally applied dc magnetic field which introduces a Zeeman splitting in CdMnTe. However, only a very small field is required since the effective Landé g-factor for electrons in dilute magnetic semiconductors is huge (\sim

100). On the other hand, the advantage of CdMnTe is that it is lattice matched to CdTe and hence interface scattering is less of a problem. It may also be advantageous to have a 5-layered quantum dot consisting of metal/magnetic semiconductor/semiconductor/ magnetic semiconductor/metal since it may be easier to inject spin coherently from a magnetic semiconductor into a semiconductor. Suffice it to say then, that it may be possible to inject an electron into one of the spin eigenstates of the semiconductor dot from spin polarized contacts. Most recently, 90% spin polarized electron injection was demonstrated from the dilute magnetic semiconductor $\text{Be}_x\text{Mn}_y\text{Zn}_{1-x-y}\text{Se}$ into GaAs at a temperature below 5 K [42] and at a relatively large magnetic field which induces a Zeeman splitting in the magnetic semiconductor. While the temperature is high enough for quantum computing applications, the applied magnetic field is too large and may flip the spin in the semiconductor quantum dot, thus corrupting the qubit. The problem of coherent spin injection from a ferromagnetic material into a semiconductor is a topic of much current research. It has a long history and success has been elusive. Currently, this is a significant challenge [43].

Another important question is how easy will it be to maintain single electron occupancy in each dot. As long as the energy cost to add an additional electron ($= e^2/2C$; C is the capacitance of the dot) significantly exceeds the thermal energy kT , only a single electron will occupy each dot. Uniform electron occupancy in arrays of $> 10^8$ dots has been shown experimentally [44].

2.2.1 Single qubit rotations

We will now describe how a selected qubit in a quantum dot can be rotated by an arbitrary angle. Note from Equation (3) that the spin-splitting of the ground state depends on the interface spin-orbit coupling coefficient α . This quantity is proportional to the interface electric field and hence can be modulated by altering the interface potential (in this case the quantum dot's interface with the surrounding insulator (Al_2O_3) is the relevant interface) by applying an electrostatic field normal to the interface. The applied electric field will also probably alter a and p_x thus contributing even more to the modulation of the spin-splitting energy. The possibility of this external electrostatic modulation was predicted by Datta and Das [37] and experimentally demonstrated by Nitta, et. al [39] who were able to vary α by a factor of 2 by varying the interface potential by 3 V. In self-assembled quantum dots whose geometry is like that in Fig. 1, we will have to apply a potential between the top contact of a dot and the bottom substrate since the sidewalls (interface with Al_2O_3) are not electrically accessible in this configuration. This is obviously not the best situation because the applied field is primarily parallel to the interface rather than perpendicular. However, there is always a small perpendicular component because of fringing effects and this will alter the spin splitting of the ground state. An alternate (but more difficult) configuration is shown in Fig. 2. The Rashba potential can be applied via lithographically defined gates which contact the insulating barriers surrounding the quantum dots. Hence, they do not induce any significant current flow and can apply the Rashba potential. These gates must be spatially resolved from ohmic contacts to the target and control dots which are required

to measure the spin orientation in these dots as described in section 2.3. This requires challenging e-beam lithography.

We can make an estimate of the spin splitting from Equation (3). Assuming that $|a| = 0.1$, $W_x = 500 \text{ \AA}$ and $\alpha = 3 \times 10^{-12} \text{ eV-m}$ [38], we find that the spin-splitting energy is $50 \mu\text{eV}$. This places a severe constraint on the temperature of operation. This computer must operate at millikelvins.

We cannot apply a large potential over a dot along the x-direction lest we overcome the Coulomb blockade and cause a current to flow between the two spin-polarized contacts. This will collapse the wavefunction by transferring the electron into the contacts which are dissipative. Current flow is allowed only when the qubit has to be read and the information in the read data is discarded thereafter (erasure). Otherwise, we must always operate within the Coulomb blockade regime to avoid dissipation. Assuming that a dot has a capacitance of 1 aF , the maximum voltage that we can apply over the dot without breaking the Coulomb blockade and inducing a current flow is 80 mV .

In order to rotate the qubit in a selected quantum dot, we will apply a potential pulse of appropriate duration to that dot which will bring the spin splitting energy in that dot in resonance with an applied global ac magnetic field B_{ac} . This resonance will then rotate the qubit placing it in a coherent superposition of the eigenspinors

$$qubit = a_{\uparrow} | \uparrow \rangle + a_{\downarrow} | \downarrow \rangle . \quad (14)$$

Thus, the desired single qubit rotation can be achieved.

2.2.2 2-qubit controlled rotation operation

To perform the operation of the 2-qubit quantum controlled rotation gate, we will require to rotate the spin in the target quantum dot (target qubit) by an arbitrary angle if, and only if, the spin in the neighboring quantum dot (control qubit) is at a specified orientation. The control qubit must remain unchanged in the process. It is obvious that the total spin splitting Δ_{target} in the target dot depends, among other things, also on the exchange interaction J with the neighboring (control) dot (and hence on the spin orientation of the control qubit) if the two dots are exchange coupled. After all, the exchange term will appear in the Hamiltonian of the coupled two-dot system. For instance, without exchange interaction, the Rashba spin splitting energy in the target dot is

$$E_{\uparrow} - E_{\downarrow} = \Delta \quad (15)$$

Now, let us turn the exchange interaction on which lowers the energy of the singlet state with respect to that of the triplet state. Thus, if the control dot's spin is pointing "up", the target dot's spin will prefer to be "down" even more than if the exchange interaction were not there. This increases Δ . On the other hand, if the control dot's spin is pointing "down", then Δ is decreased. The energy levels are shown in Fig. 3. Thus, the potential

V_{target} that brings the *total* spin splitting energy Δ_{target} in the target dot in resonance with the ac magnetic field B_{ac} depends on the spin orientation in the control dot. Herein lies the possibility of conditional dynamics. We can find the V_{target} that will rotate the target qubit through an arbitrary angle only if the control qubit is in the specified orientation. Application of this potential V_{target} to the target dot realizes the operation of a quantum controlled rotation gate.

To turn the exchange “on” and “off”, one can apply a differential potential between the target and control dots which will skew the wavefunctions and change the overlap between the wavefunctions of the target and control electrons. Alternately, one can apply positive potentials to *all* Rashba contacts A , A' , A_1 and A_2 . Since there is no differential potential, the Rashba effect is not modified, but the positive potential will attract the electrons into the insulating layers surrounding the quantum dots, thus increasing the overlap between the wavefunctions and the exchange interaction.

2.3 Spin measurement

After quantum computation is over, we need to read the result by measuring the qubits. During this process, the qubits will collapse to classical bits. These classical bits are the measured spin orientations in relevant dots. They are measured by measuring the current that results when the potential over the dot is raised over the Coulomb blockade threshold. If we assume that the differential phase-shift suffered by the spin in traversing the dot is negligible; in other words, transport through the dot does not rotate the spin, then the magnitude of the measured current can tell us the spin orientation [37]. It was shown in ref. [37] that the spin-polarized contacts act as electronic analogs of optical polarizers and analyzers, so the current will depend on the projection of the spin of the quantum dot’s resident electron on the spin orientation in the contacts. Thus, by measuring the current, we can tell the spin orientation in any quantum dot.

2.4 Calibration

For each dot, the potential V that needs to be applied to flip the spin by bringing the dot in resonance with B_{ac} can be calibrated following the procedure outlined by Kane [25]. With $B_{ac} = 0$, we measure the spin in a quantum dot. Then we switch on B_{ac} and sweep V over a range. Next B_{ac} is switched off and the spin is measured. The range of V is progressively increased till we find that the spin has flipped. We then proceed to narrow the range with successive iteration while making sure that the spin does flip in each iteration. Finally this allows us to ascertain V with an arbitrary degree of accuracy. As pointed out by Kane [25], the calibration procedure can, in principle, be carried out in parallel over several dots simultaneously and the voltages stored in adjacent capacitors. External circuitry will thus be needed only to control the timing of the biases (application of V_{target}) and not their magnitudes. While this is definitely an advantage, fabricating nanoscale capacitors adjacent to each individual dot is outside the scope of self-assembly. Moreover, capacitors discharge

over time, requiring frequent recalibration through refresh cycles, so that this may not be a significant advantage.

2.5 Input and Output Operations

Any computer is of course useless unless we are able to input and output data successfully. Since we are using spin-polarized contacts to inject an electron in each dot, we know the initial orientation. Those dots where the initial orientation is the one we want are left unperturbed while the spins in the remaining dots are flipped by resonating with B_{ac} . This process prepares the quantum computer in the initial state for a computation and can be viewed as the act of “writing” the input data. Computation then proceeds on this initial state by carrying out a desired sequence of controlled rotation operations. Reading the data is achieved as described in subsection 2.3.

2.6 Comparisons with similar proposals

Proposals similar to that presented in this paper, which envision nanoelectronic spin-based implementations of universal quantum gates, have been forwarded in the past by Privman [26], Kane [25] and more recently by Vrijen, at. al. [27]. Our proposal is distinct from those previous versions in many ways. The first two of the previous proposals envision qubits as being encoded by nuclear spins and a delicate transduction between electron- and nuclear-spins is required for data communication. Both Vrijen and we have eliminated the role of nuclear spins (and the need for coupling between electron and nuclear spins), but perhaps at the cost of a somewhat smaller T_2 time (spin coherence time). The major difference between our proposal and all others is that we do not need any dc magnetic field at all. All previous versions split the spins using the Zeeman effect induced by a strong dc magnetic field. We use the Rashba effect instead (which is purely electrostatic). Since we only need a small ac magnetic field (supplied by a microwave source), there is some hope of a “lightweight” implementation where heavy electro-magnets for generating strong dc magnetic fields are not required. There is nonetheless a cryogenic requirement which is the main obstacle to realizing a truly “portable” quantum computer. This obstacle is not easy to overcome.

Another major difference with previous proposals is that our structure can be mostly self-assembled thus eliminating the requirement of performing Herculean feats in lithography. In the next section, we briefly describe how it may be possible to self-assemble a quantum computer.

3 Self Assembly

The self-assembly process that we propose is relatively standard and has been successfully applied by a number of groups, including us, for fabricating ordered two-dimensional arrays of quantum dots or nanowires [45]. The synthesis proceeds as follows.

First an Al foil is dc anodized in 15% sulfuric acid for several hours with a current density of 40 mA/cm². This produces a nanoporous alumina film on the surface of the foil with a quasi-ordered arrangement of pores. The film is stripped off and the foil is re-anodized for a few minutes. The alumina film that forms on the surface after the second anodization step has a very well ordered arrangement of nanopores [46]. Fig. 4 shows a raw atomic force micrograph of pores formed by anodizing in oxalic acid. The pore diameter is 52 nm and the thickness of the wall separating two adjacent pores is of the same order. If the anodization is carried out in sulfuric acid, the pores that self-assemble have a much smaller diameter of 10 ± 1 nm with a wall thickness of the same order [45]. Cross-section TEM of the pores have revealed that they are cylindrical with very uniform diameter along the length. The length of the pores is of course the thickness of the alumina film and depends on the duration of anodization. Typically, the length is a few thousands of angstroms.

Multilayered quantum dots as shown in Fig. 1 are formed by sequentially electrodepositing the constituent layers selectively within the pores. However, in order to have appreciable overlap of the wavefunctions in neighboring dots for exchange coupling, we must first decrease the thickness of the alumina walls separating two adjacent dots. The separation can be decreased to as small as ~ 1 nm by widening the pores. This is accomplished by soaking the porous alumina film in phosphoric acid which dissolves the alumina from the walls of the pores.

Electrodeposition of the constituent layers of a multi-layered quantum dot (or quantum dash) is carried out in steps. In Fig. 1(a), we show a trilayered dot of Fe-GaAs-Fe where Fe acts as the spin polarized material. We recognize that this may not be the optimal combination, but at least this interface is known to be sharp and has been well characterized in the past [47]. For depositing the first Fe layer, the alumina film is immersed in a solution of FeSO_4 and an ac signal of 20 V rms amplitude and 250 Hz frequency is imposed between the aluminum substrate and a graphite counter electrode. During the cathodic half cycle of the ac signal, the Fe^{++} ion is reduced to zero-valent Fe metal which goes into pores selectively since they offer the least impedance path for the ac current to flow. Since alumina is a valence metal oxide, the zero-valent Fe is not re-oxidized to Fe^{++} during the anodic half-cycle. After a few seconds of electrodeposition, we are left with a ~ 10 -nm layer of Fe at the bottom of the pore [48].

The partially filled alumina film is then ac electrolysed in arsenic acid for a few seconds which leaves behind the As^{---} ions adsorbed on the walls of the pores. Next, the sample is immersed in a boiling aqueous solution containing the Ga^{+++} ion. The Ga^{+++} ion reacts with the As^{---} in the walls of the pore to produce a ~ 10 -nm thick layer of GaAs on top of the Fe layer. Finally, another ~ 10 -nm thick layer of Fe is deposited on top. This results in the structure of Fig. 1(a). Note that the spin-polarized contacts (Fe) are automatically *self-aligned* to the semiconductor dot (GaAs) in this approach.

If we wish to self-assemble the alternate structure in Fig. 1(b), we will use telluric acid instead of arsenic acid for the ac electrolysis. CdMnTe is deposited by immersing the alumina film in a boiling solution of CdSO_4 and MnSO_4 , whereas CdTe is deposited by immersing in

a solution of pure CdSO_4 .

It should be pointed out that one is not limited by material. Almost anything can be deposited selectively within the pores, one way or another. Even silicon can be deposited by slow deposition using molecular beam epitaxy and Group V elements like carbon have been deposited within the pores employing essentially gas-phase epitaxy [49]. Plasma-enhanced chemical vapor deposition is another promising approach.

Material purity is of extreme concern in any electrochemical synthesis. Chemical reagents are never very pure and we certainly do not want a magnetic impurity in the semiconductor dot that will tend to cause unwanted spin flips. Since it is possible to fill the pores using very slow deposition in an MBE set-up, one could use this approach to guarantee vastly improved material purity with a commensurate increase in fabrication cost.

3.1 Wiring the gates to make a computer

Arbitrary electrical connections will have to be made between different gates in order to make a computer. The lithographic challenge associated with this task is daunting; however, there is an alternate. We can deposit Au over the top Fe contact in the same way as we deposit Fe itself. Gold sulfide is an appropriate electrochemical source for gold. Conjugated organic molecules such as biphenyl dithiol and gold clusters can be co-evaporated on the surface after each pore is sealed with a top Au layer. The end-group in the organic molecule self-attaches to Au acting as “alligator-clips” [50, 51]. The molecules bridged by Au clusters (Fig. 5a) are electrically conducting with a resistance of 10-40 $\text{M}\Omega$ per molecule [52, 53]. They are called “molecular ribbons” and provide *self-assembled* electrical connection between the quantum dots (Fig. 5a) [54]. However, the connection exists between every dot and hence must be surgically modified to realize a specific interconnection pattern. For this purpose, one will need to remove the unwanted connections with an STM tip. This is a slow and laborious process but still beats lithography.

The elecrical interconnects transmit electrical signals such as Rashba voltages and spin currents. However, they do not transport quantum signal such as the state of spin polarization. For this purpose, we need “spin wires” which transmit quantum information about spin polarization. Fortunately, making “spin wires” is somewhat easier. A line of exchange coupled quantum dots is a “spin wire” since its ground state is anti-ferromagnetic [55, 56] so that the spin repeats itself every other dot. This allows spin state to be transmitted down a line consisting of an odd number of dots. Such a spin wire is shown in Fig. 5b. Unfortunately such wires are not “unidirectional” and do not transmit signal (spin orientation) from the input end to the output end unidirectionally [55, 57]. We had shown in ref. [57] that unidirectionality in time effectively also imposes unidirectionality in space. Temporal (and consequently spatial) unidirectionality can be achieved by sequential clocking (this is the technique adopted to transmit charge packets in conventional charge coupled devices [58]). We turn the exchange interaction between neighboring dots “on” sequentially by propagating a positive pulse down a line connected to contacts interposed between adjacent dots as shown in Fig. 5(b).

The above lines will have to be delineated by lithography. However, since much of the pattern is periodic, it may be possible to use techniques such as achromatic interferometric x-ray lithography which have a much faster throughput than direct write lithography to delineate the clocking connections. Direct writing is not completely unavoidable, however. Connections to the external world for data input/output to the entire chip must be delineated with direct-write lithography. This is however not as demanding as making all the internal connections (dot-to-dot connections) with lithography.

4 Conclusions

In this paper, we foresee the application of a great advance in materials technology, nanoscale self-assembly, to realize a great advance in information technology - the quantum computer. Past proposals of semiconductor implementations of quantum computers [25, 27] required extremely challenging fabrication methodologies and at least some of them relied on delicate interaction between nuclear and electron spins to transduce the qubit into a measurable signal. The present paradigm is much simpler, probably more robust, and the possibility of self-assembly makes it very attractive.

5 Acknowledgement

I am indebted to many individuals for insightful discussion, but especially to Profs. P. F. Williams and D. J. Sellmyer.

References

- [1] B. Schumacher, *Phys. Rev. A*, **51**, 2738-2747 (1995).
- [2] A. Steane, *Rep. Prog. Phys.*, **61**, 117-173 (1998).
- [3] P. W. Shor, in *Proc. 35th. Ann. Symp. Foundations of Computer Science*, Ed. S. Goldwasser, pp. 124-134 (IEEE Computer Society, Los Alamitos, CA, 1994).
- [4] L. K. Grover, *Phys. Rev. Lett.*, **79**, 325-328 (1997); L. K. Grover, *Phys. Rev. Lett.*, **79**, 4709-4712 (1997).
- [5] D. P. DiVincenzo, *Phys. Rev. A*, **51**, 1015-1021 (1995).
- [6] S. Lloyd, *Phys. Rev. Lett.*, **75**, 346-349 (1995).
- [7] A. Barenco, *Proc. R. Soc. London*, **A449**, 679-683 (1995).
- [8] P. W. Shor in *Proc. 37th Ann. Symp. Foundations of Comp. Sci.*, IEEE Computer Society Press, pp. 56-65 (1996).
- [9] A. Kitaev, *Russian Math Surveys*, **52**, 1191 (1997).
- [10] P. O. Boykin, T. Mor, M. Pulver, V. Roychowdhury and F. Vatan, LANL e-print quant-ph #9906054.
- [11] A. R. Calderbank and P. W. Shor, *Phys. Rev. A*, **54**, 1098-1105 (1996).
- [12] J. I. Cirac and P. Zoller, *Phys. Rev. Lett.*, **74**, 4091-4094 (1995).
- [13] Q. A. Turchette, C. J. Hood, W. Lange, H. Mabuchi and H. J. Kimble, *Phys. Rev. Lett.*, **75**, 4710-4713 (1995).
- [14] C. Monroe, D. M. Meekhof, B. E. King, W. M. Itano and D. J. Wineland, *Phys. Rev. Lett.*, **75**, 4714-4717 (1995).
- [15] D. G. Cory, A. F. Fahmy T. F. and Havel, in *Proc. 4th Workshp. on Physics and Computation*, (Complex Systems Institute, Boston, MA, 1996). See also, D. G. Cory, M. G. Price and T. F. Havel, *Proc. Natl. Acad. Sci., USA*, **94**, 1634-1639 (1997).
- [16] N. A. Gershenfeld and I. L. Chuang, *Science*, **275**, 350-356 (1997).
- [17] J. A. Jones and M. Mosca, *Phys. Rev. Lett.*, **83**, 1050-1053 (1999).
- [18] S. L. Braunstein, C. M. Caves, R. Josza, N. Linden, S. Popescu and R. Schack, *Phys. Rev. Lett.*, **83**, 1054-1057 (1999).
- [19] P. Mohanty, E. M. Q. Jariwalla and R. A. Webb, *Phys. Rev. Lett.*, **78**, 3366-3369 (1997).

- [20] A. Barenco, D. Deutsch and A. Ekert, *Phys. Rev. Lett.*, **74**, 4083-4087 (1995).
- [21] S. Bandyopadhyay, A. Balandin, V. P. Roychowdhury and F. Vatan, *Superlat. Microstruct.*, **23**, 445-464 (1998).
- [22] A. Balandin and K. L. Wang, *Superlat. Microstruct.*, **25**, 509 (1999).
- [23] J. Preskill, *Proc. Royal Soc. London A*, **454**, 385 (1998).
- [24] G. Feher, *Phys. Rev.*, **114**, 1219 (1959).
- [25] B. E. Kane, *Nature* (London), **393**, 133-137 (1998).
- [26] V. Privman, I. D. Vagner and G. Kvetsel, *Phys. Lett. A*, **239**, 141 (1998).
- [27] R. Vrijen, E. Yablonovitch, K. Wang. H. W. Jianh, A. Balandin, V. Roychowdhury, T. Mor and D. DiVincenzo, LANL e-print quant-ph #9903042.
- [28] J. M. Kikkawa and D. D. Awschalom, *Phys. Rev. Lett.*, **80**, 4313 (1998).
- [29] R. Romestain, S. Geschwind and G. E. Devlin, *Phys. Rev. Lett.*, **39**, 1583 (1977).
- [30] H. Benisty, C. M. Sotomayor-Torres and C. Weisbuch, *Phys. Rev. B*, **44**, 10945 (1991).
- [31] W. G. Unruh, *Phys. Rev. A*, **51**, 992 (1995).
- [32] S. Bandyopadhyay and V. P. Roychowdhury, *Superlat. Microstruct.*, **22**, 411 (1997).
- [33] D. Loss and D. P. DiVincenzo, *Phys. Rev. A*, **57**, 120 (1998).
- [34] M. Oestreich, J. Hübner, D. Hägele, P. J. Klar, W. Heimbrodt, W. W. Rühle, D. E. Ashenford and B. Lunn, *Appl. Phys. Lett.*, **74**, 1251-1253 (1999).
- [35] E. I. Rashba, *Sov. Phys. Semicond.*, **2**, 1109-1122 (1960); Y. A. Bychkov and E. I. Rashba, *J. Phys. C*, **17**, 6039-6045 (1984).
- [36] G. Lommer, F. Malcher, and U. Rössler, *Phys. Rev. Lett.*, **60**, 728-731 (1988).
- [37] S. Datta and B. Das, *Appl. Phys. Lett.*, **56**, 665-667 (1990).
- [38] B. Das, D. C. Miller and S. Datta, *Phys. Rev. B*, **39**, 1411 (1989).
- [39] J. Nitta, T. Akazaki, H. Takayanagi, and T. Enoki, *Phys. Rev. Lett.* **78**, 1335-1339 (1997).
- [40] L. H. v. Leuken and R. A. d. Groot, *Phys. Rev. B*, **51**, 7176 (1995); J. M. D. Coey, A. E. Berkowitz, Ll Balcells, F. F. Putris and A. Barry, *Phys. Rev. Lett.*, **80**, 3815 (1998).
- [41] Y. Ohno, D. K. Young, B. Beschoten, F. Matsukura, H. Ohno and D. D. Awschalom, *Nature* (London), **402**, 790 (1999).

[42] R. Fiederling, M. Keim, G. Reuscher, W. Ossau, G. Schmidt, A. Waag and L. W. Molenkamp, *Nature* (London), **402**, 787 (1999).

[43] H. X. Tang, F. G. Monzon, Ron Lifshitz, M. C. Cross and M. L. Roukes, *Phys. Rev. B*, **61**, 4437 (2000).

[44] B. Muerer, D. Heitman and K. Ploog, *Phys. Rev. Lett.*, **68**, 1371 (1988).

[45] See, for example, S. Bandyopadhyay, A. E. Miller, H-C Chang, G. Banerjee, V. Yuzhakov, D-F Yue, R. E. Ricker, S. Jones, J. A. Eastman, E. Baugher and M. Chandrasekhar, *Nanotechnology*, **7**, 360-371 (1996) and references therein.

[46] H. Masuda and M. Satoh, *Jpn. J. Appl. Phys.*, **35**, L126 (1996).

[47] See, for example, G. A. Prinz, *Physics Today*, **48**, 58 (1995).

[48] L. Menon, M. Zheng, H. Zeng, Sellmyer and S. Bandyopadhyay, in *Advanced Luminescent Materials and Quantum Confinement*, Eds. M. Cahay, S. Bandyopadhyay, D. J. Lockwood, N. Koshida, J-P Leburton, M. Meyyappan and T. Sakamoto (The Electrochemical Society, Inc., Pennington, New Jersey, 1999), pp. 413-424.

[49] J. Li, C. Papadopoulos, J. M. Xu and M. Moskovitz, *Appl. Phys. Lett.*, **75**, 367 (1999).

[50] J. M. Tour and J. S. Schumm, *Polym. Prepr.*, **34**, 368 (1993).

[51] J. I. Henderson, S. Feng, G. M. Ferrence, T. Bein and C. P. Kubiak, *Inorg. Chim. Acta*, **242**, 115 (1996).

[52] R. P. Andres, T. Bein, M. Dorogi, S. Feng, J. I. Henderson, C. P. Kubiak, W. J. Mahoney, R. G. Osifchin and R. Reifenberger, *Science*, **272**, 1323 (1996).

[53] R. P. Andres, J. D. Bielefeld, J. I. Henderson, D. B. Janes, V. R. Kolagunta, C. P. Kubiak, W. J. Mahoney and R. G. Osifchin, *Science*, **273**, 1690 (1996).

[54] S. Datta, D. B. Janes, R. Andres, C. P. Kubiak and R. Reifenberger, *Semicond. Sci. Technol.*, **13**, 1347 (1998).

[55] S. Bandyopadhyay, B. Das and A. E. Miller, *Nanotechnology*, **5**, 113 (1994).

[56] S. N. Molotkov and S. S. Nazin, *JETP Lett.*, **62**, 272 (1995).

[57] S. Bandyopadhyay and V. P. Roychowdhury, *Jpn. J. Appl. Phys.*, Pt. 1, **35**, 3350 (1996).

[58] D. K. Schröder, *Advanced MOS Devices*, Modular Series on Solid State Devices, Vol. VII, Eds. R. F. Pierret and G. W. Neudeck, (Addison Wesley, Reading, Massachusetts, 1988).

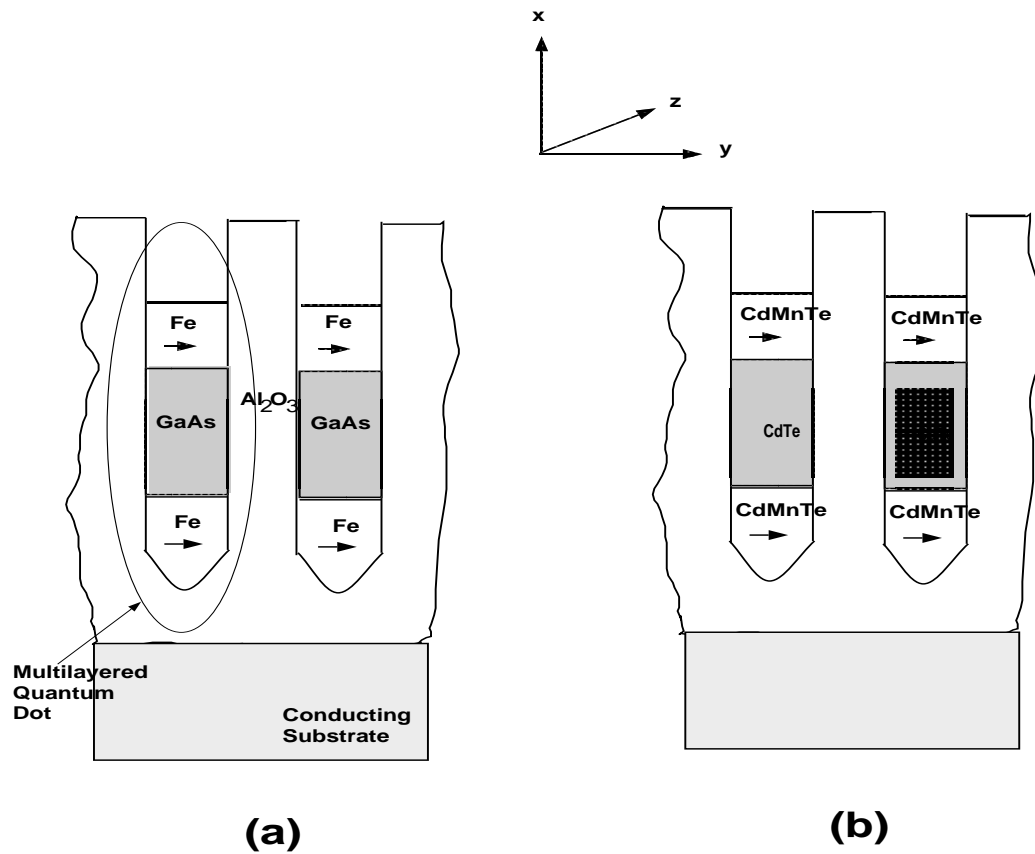


Figure 1: Two multilayered quantum dots (or quantum dashes) separated by an insulating barrier. Each dot or dash consists of a semiconductor sandwiched between two self-aligned spin polarized contacts. This structure can be electrochemically self-assembled. (a) Fe-GaAs-Fe and (b) CdMnTe-CdTe-CdMnTe.

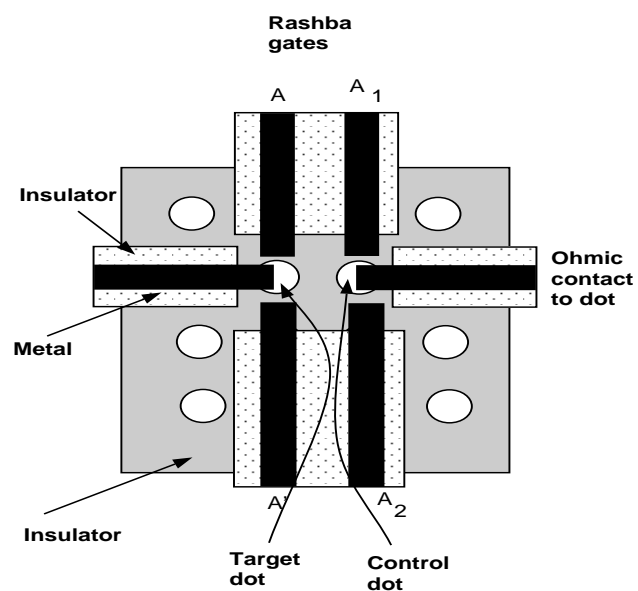


Figure 2: Layout of the Rashba gates and the ohmic contacts used for spin injection and detection. Top view.

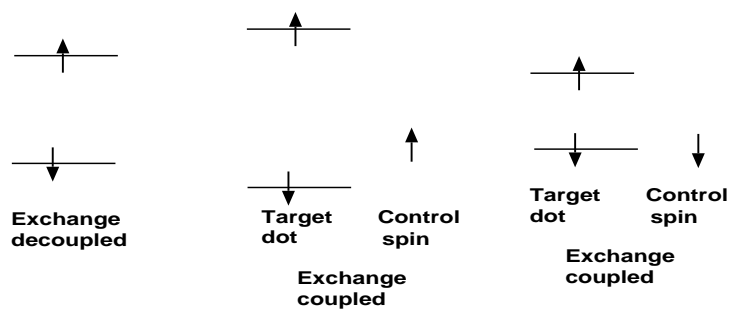


Figure 3: Energy levels in the target quantum dot depending on the spin orientation in the control dot.

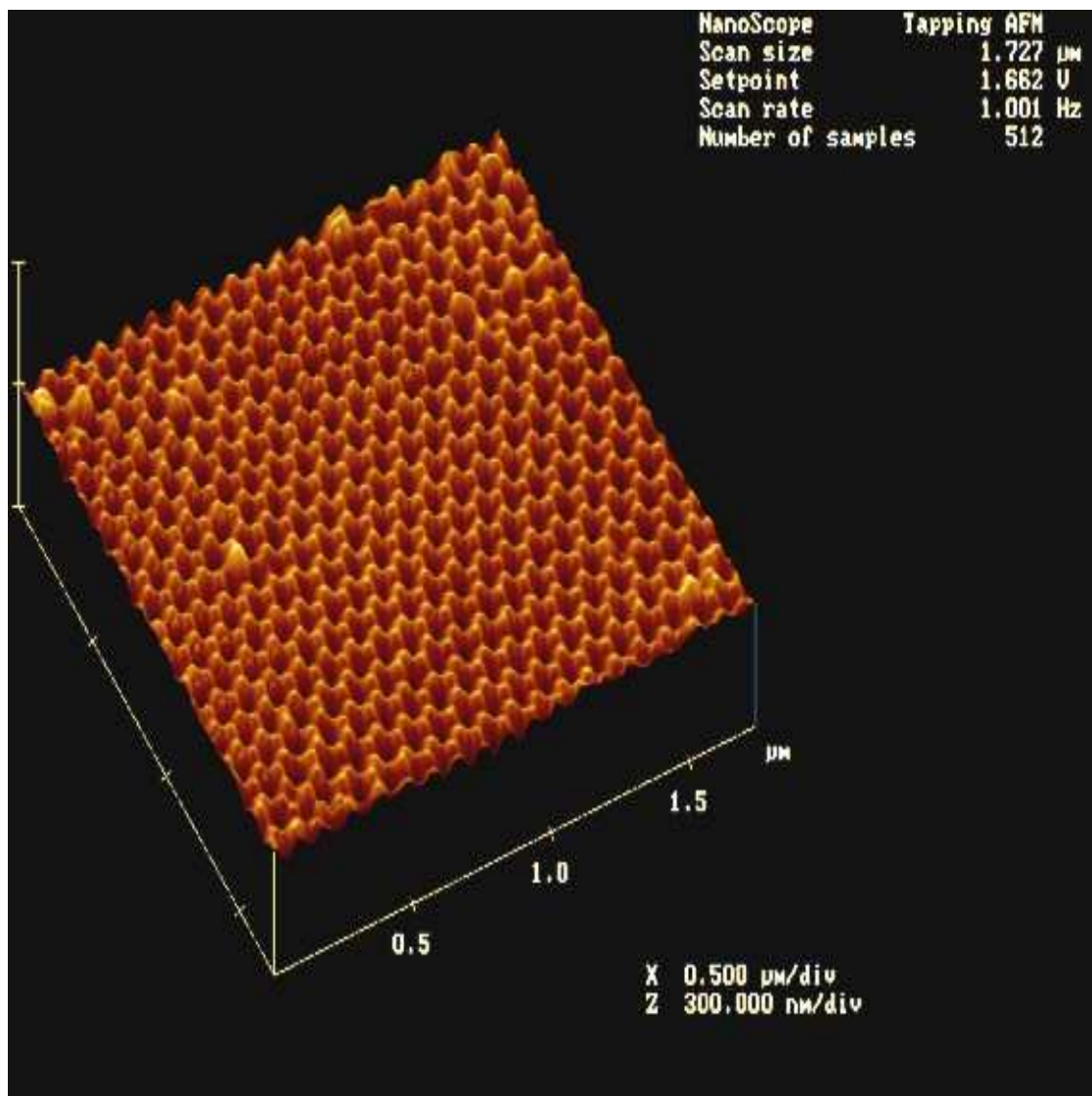


Figure 4: Raw atomic force micrograph of pore morphologies produced by anodization of an aluminum foil in oxalic acid. The average pore diameter is 52 nm with a 5% standard deviation. This structure acts as a self-assembled template for self-assembling a quantum computer.

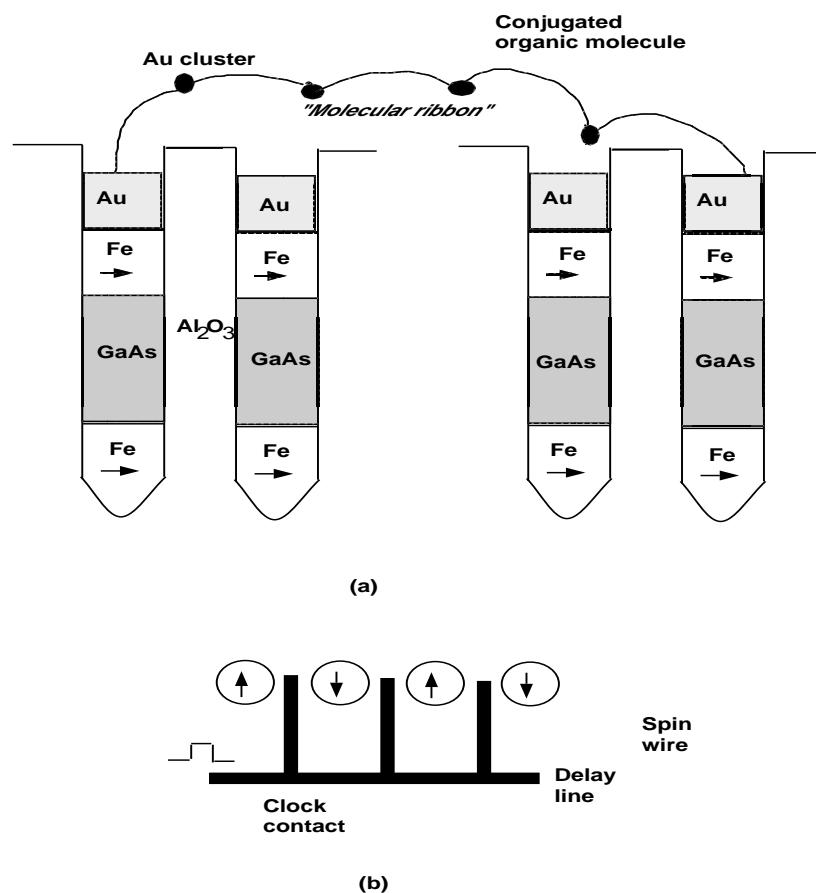


Figure 5: Wiring the quantum computer. Dot-to-dot connections are self-assembled using conjugated organic molecules with appropriate end-groups that self-adhere to gold. Gold clusters act as links in the bridge. Every Au contact is connected to others via the linked molecules and the unwanted connections are subsequently removed with an STM tip.